

Research article

A necroptosis-regulated model from single-cell analysis that predicts survival and identifies the Pivotal role of MAGEA6 in hepatocellular carcinoma

Youcheng Zhang^{a,c,1}, Dapeng Chen^{a,1}, Bing Ang^{b,1}, Xiyue Deng^a, Bing Li^c, Yi Bai^d, Yamin Zhang^{d,*}

^a The First Central Clinical School, Tianjin Medical University, Tianjin, 300192, China

^b Department of Oncology, Tianjin First Central Hospital Clinic Institute, Tianjin 300192, China

^c Department of Pediatric Surgery, Huai'an Maternal and Child Health Care Center, Huai'an, 223001, Jiangsu Province, China

^d Department of Hepatobiliary and Pancreatic Surgery, Tianjin First Central Hospital, School of Medicine, Nankai University, Tianjin, 300192, China

ARTICLE INFO

Keywords:

Hepatocellular carcinoma

Necroptosis

Prognostic signature

Single-cell

ABSTRACT

Objective: Hepatocellular carcinoma (HCC) ranks as the third leading cause of cancer-related deaths, constituting 75%–85 % of all primary liver cancers. The objective of this study was to develop a necroptosis-related gene signature using single-cell and bulk RNA sequencing to predict HCC patient prognoses.

Methods: A total of 25 key necroptosis regulators were identified from previous literature. We evaluated the necroptosis scores of different cell types using single-cell sequencing data from HCC and analyzed 168 necroptosis-related genes. The Cancer Genome Atlas Liver Hepatocellular Carcinoma (TCGA-LIHC) dataset served as the training set for establishing a novel necroptosis-related gene risk signature, employing univariate and multivariate Cox regression analyses. Additionally, the study examined the model's relevance in immunity and immunotherapy, and predicted chemosensitivity in HCC patients based on the gene signature. The key genes were validated by the biological experiments.

Results: Compared to other cell types, hepatoma cells displayed the lowest necroptosis scores. A new six-gene necroptosis-related signature (S100A11, MAGEC2, MAGEA6, CTP2C9, SOX4, AKR1B10) was developed using the TCGA database and validated in the ICGC database. Patients in the high-risk category had poorer prognoses, with the risk score serving as an independent prognostic indicator beyond other clinical factors. These high-risk patients also exhibited greater immune infiltration but demonstrated a weaker anti-tumor response due to elevated expression of immune checkpoints. Pathways involving hypoxia, glycolysis, and P53, as well as the frequency of P53 somatic mutations, were notably heightened in the high-risk group. Additionally, the six genes in the model showed significantly different mRNA expression in hepatoma cell lines compared to normal hepatocytes, with the role of MAGEA6 in liver cancer being elucidated through critical experiments.

* Corresponding author. Department of Hepatobiliary and Pancreatic Surgery, Tianjin First Central Hospital, School of Medicine, Nankai University, WenZheng Road, XiQing District, Tianjin, China.

E-mail address: 5020200824@nankai.edu.cn (Y. Zhang).

¹ These authors contributed equally to this work.

<https://doi.org/10.1016/j.heliyon.2024.e37711>

Received 25 June 2024; Received in revised form 2 September 2024; Accepted 9 September 2024

2405-8440/© 2024 Published by Elsevier Ltd. This is an open access article under the CC BY-NC-ND license (<http://creativecommons.org/licenses/by-nc-nd/4.0/>).

Conclusions: This study successfully developed a six-gene necroptosis-related signature to predict prognoses in HCC patients. It further explored the roles of necroptosis in hepatoma cells and the tumor microenvironment.

1. Instruction

In terms of cancer incidence and mortality rates, hepatocellular carcinoma (HCC) ranks first, accounting for 75%–85 % of all primary liver cancer patients [1]. In 2018, it was estimated that there were 9.3 new cases of liver cancer worldwide per 100,000 people, with an 8.5 death rate [2]. Currently, researchers are still investigating the mechanisms of tumorigenesis and progression. Treatment options available for advanced-stage patients are very limited [3]. According to the mainstream hypothesis, tumorigenic factors cause genetic mutations in somatic cells, which contributes to the derangement of normal genes and disruption of gene expression, resulting in the formation of tumor cells with morphology, metabolism, and function different from normal cells [4]. The approach to treating cancers has now progressed to precision medicine, which incorporates the patient's treatment plan with the cancer's molecular characteristics, such as tumor mutational burden (TMB), microsatellite instability (MSI), and programmed cell death protein 1 (PD1) expression level. Patients with advanced HCC can only hope for targeted therapy and immunotherapy because curative treatments such as surgical resection, or liver transplantation are not options. However, a limited proportion of HCC patients can undergo clinical remission from targeted therapy and immunotherapy, and many acquire drug resistance [5,6]. Therefore, precise diagnosis and individualized treatment strategies are necessary to achieve precision medicine for HCC patients. Research on novel biomarkers is urgently needed to help in early clinical diagnosis, risk assessment, and therapy effectiveness evaluation.

One of the most crucial characteristics of cancer is the evasion of cell death [7]. To address this problem, researchers believe that novel therapy that circumvents the apoptotic pathway will be effective. Emerging research has revealed connections between anti-tumor immunity and non-apoptotic regulated cell death. Particularly, anti-cancer immune responses are synergistically induced by autophagy, necroptosis, pyroptosis, paraptosis, and ferroptosis, while simultaneously possibly being inhibited by these processes [8]. Necroptosis is a caspase-independent necrotic cell death that is primarily mediated by receptor-interacting protein [RIP] kinase 1 (RIPK1), RIPK3, and mixed lineage kinase domain-like pseudokinase (MLKL) [9]. Necroptosis, a distinct form of programmed cell death, can overcome apoptosis resistance and activate and boost anti-tumor immunity. Necroptosis in tumor has a complex biological mechanism. Crucial necroptosis regulators frequently exhibit downregulated expression in tumor cells [10,11], revealing that tumor cells could survive by avoiding necroptosis. However, expression levels of these essential mediators are increased in some forms types of cancer [12]. For instance, more immunostimulatory cytokines were released in the tumor microenvironment (TME) due to RIPK3 activation-dependent derepression of TRIM28 in cancer cells, which helps promote effective anti-tumor immunity [13]. However, RIPK1 was discovered to be upregulated in glioblastoma and was associated with a bad outcome via inhibiting p53 activation [14]. As a result, necroptosis may trigger a robust adaptive immune response that prevents tumor growth; The induced inflammatory response, however, can encourage carcinogenesis and cancer spread, so necroptosis might produce an immunosuppressive TME [15]. Immunotherapy is also greatly influenced by the altered immune microenvironment caused by necroptosis [16]. Therefore, it is crucial to investigate how necroptosis affects HCC.

Even though numerous studies have shown the significance of necroptosis in HCC, the precise mechanism is still unknown. According to the latest research, tumor-infiltrating lymphocytes (TILs), more specifically CD8⁺ T cells, accumulated in tumors with increased expression of genes related to necroptosis. Furthermore, the expression value of RIPK1, RIPK3, and MLKL-p was related to improved prognosis [17]. However, increased necroptosis in the liver is related to aging, which promotes chronic inflammation of the liver, leading to hepatic fibrosis and disease, including liver cancer [18]. Additionally, Heparanase could promote HCC metastasis by inducing necroptosis in microvascular endothelial cells [19]. Prognostic models based on ribonucleic acid (RNA) sequencing have made significant advances as high-throughput sequencing has expanded. The prognostic model built by necroptosis-related genes may potentially result in new treatment options in addition to improving prognosis prediction of HCC patients [20,21]. In this work, we combined bulk RNA and single-cell sequencing to analyze necroptosis genes and found that hepatoma cells had the lowest necroptosis score compared to other cell types, suggesting that hepatoma cells can escape necroptosis. We further identified genes associated with necroptosis in HCC. Researchers developed a prognostic signature based on necroptosis-related genes that could precisely forecast the outcome of HCC patients and recommend immunotherapeutic treatment. In addition, we investigated the significance of prognostic models in immune function and immunotherapy. The association between prognostic models and several pathways, including the P53 and apoptosis, was also investigated.

2. Methods and materials

2.1. Data acquisition

We obtained bulk RNA sequencing data and associated clinical information from three databases: the Cancer Genome Atlas (TCGA), the International Cancer Genome Consortium (ICGC, LIRI-JP), and the GEO14520 database. These databases provided 424 (comprising 374 tumor and 50 adjacent normal tissues), 231 tumor samples, and 220 tumor samples, respectively. Patients lacking survival data were excluded. Concurrently, we accessed single-cell RNA sequencing data from GSE149614 [22], which encompassed 10 tumor and 7 normal tissues. Given our research's emphasis on the heterogeneity of the Tumor Microenvironment (TME) in tumor

and peri-tumor tissues, we selected seven pairs of tumor and normal samples for analysis.

2.2. Single cell analysis

All single cells were enrolled in the quality control process performed by the Seurat R package [23]. Cells were included in the analysis if they met the following criteria: (a) RNA count range between 200 and 500, and (b) mitochondrial gene expression below 5 %. This resulted in the analysis of 55,341 cells, comprising 26,660 cells derived from tumors and 28,681 from normal tissues. Data normalization was performed using the "LogNormalize" algorithm with a scale factor of 10,000. The impact of Unique Molecular Identifiers (UMIs) and mitochondrial content percentages were mitigated using Seurat's ScaleData function. The Harmony R package was employed to eliminate batch effects. For cell clustering and t-Distributed Stochastic Neighbor Embedding (t-SNE) visualization, the top 30 principal components and the 2000 most variable genes were chosen [24]. Cell cluster-specific marker genes were identified using the FindAllMarkers function, and cell types were annotated based on canonical marker genes documented in prior studies (refer to Table S1).

2.3. The Acquisition of necroptosis-related genes by scRNA-seq

Table S2 represents the twenty-five key necroptosis regulators that were extracted from earlier reviews [15,25]. Utilizing twenty-five essential necroptosis regulators, we computed the necroptosis-related scores for each cell using the AddModuleScore function in the Seurat R package. Notably, hepatoma cells exhibited the lowest necroptosis scores. We subsequently isolated these cells for further examination and observed that, apart from those in cluster 1, all hepatoma cells consistently showed low necroptosis scores. This led us to identify differentially expressed genes (DEGs) between hepatoma cells from cluster 1 and those from other clusters, using the FindAllMarkers function. These DEGs are hypothesized to be associated with necroptosis in HCC.

2.4. Construction of a prognostic signature associated with necroptosis

Our analysis commenced by intersecting 168 differentially expressed genes (DEGs) with genes sequenced in the ICGC-LIHC and GEO14520 datasets. We then examined the expression levels of 125 overlapping DEGs between tumor and normal tissues in the TCGA cohort, identifying 38 DEGs that exhibited significant differential expression ($P < 0.05$, log fold change > 1). The TCGA LIHC cohort served as a training set, integrating the gene expression matrix of these 38 DEGs with survival status and duration. A univariate Cox regression analysis, conducted using the survival R package, determined the predictive relevance of these 38 DEGs. Briefly, univariable Cox regression analyses were conducted to screen DEGs with prognostic significance for inclusion in the multivariable model, using a liberal p -value threshold of < 0.10 . Then, a multivariable Cox proportional hazards model was built using a forward stepwise approach. At each step, the model automatically assessed the statistical significance ($p < 0.05$) of each variable and decided whether to retain or remove it from the model.

The regression coefficients, hazard ratios, and 95 % confidence intervals were reported for each predictor variable in the final Cox model.

2.5. Evaluation and Validation of the risk model

The risk score for each patient was calculated in both the training (TCGA) and testing (ICGC) sets, with patients divided into high- and low-risk groups based on the median risk score. Survival rates of these groups were compared using Kaplan-Meier curves. Additionally, Receiver Operating Characteristic (ROC) curve analysis was conducted to assess the predictive accuracy of the model in both sets. Further, univariate and multivariate Cox regression analyses were performed to evaluate whether the risk score independently predicted the prognosis of hepatocellular carcinoma (HCC) patients, considering factors such as tumor size, stage, age, grade, gender, and risk score. We also explored the association between the risk score and clinical characteristics, including tumor size, stage, gender, and grade.

2.6. Function enrichment analysis

The immune function scores of each patient were calculated using the GSVA R package. We then assessed the average expression levels of immune checkpoints in both high- and low-risk groups, with a significance threshold set at $P < 0.05$. Gene Set Enrichment Analysis (GSEA) was employed to identify enriched gene sets within these groups. We sourced the 50 hallmark gene sets from MsigDB (<https://www.gsea-msigdb.org/gsea/index.jsp>). Additionally, Gene Ontology (GO) pathway enrichment analysis and Kyoto Encyclopedia of Genes and Genomes (KEGG) analysis for the differentially expressed genes (DEGs) were conducted using the clusterProfiler R package [26]. The functions of DEGs were further explored using Metascape (<http://metascape.org>), an advanced online tool for gene function annotation.

2.7. Evaluation of Tumor Mutation Burden and Drug Sensitivity

Tumor Mutation Burden (TMB) was computed utilizing somatic mutation data from the TCGA datasets, with comparative analyses performed between the low- and high-risk subsets. The "maftools" R package facilitated the creation of waterfall plots, illustrating the

variance in gene mutation characteristics between these subsets. We also investigated the combined impact of TMB and risk score on the survival of hepatocellular carcinoma (HCC) patients. Drug sensitivities were assessed using the pRRophetic R package, which calculates the half-maximal inhibitory concentration (IC50) of various drugs, thereby determining the differential drug sensitivities in high-versus low-risk groups.

2.8. Cell culture

Human hepatocellular carcinoma (HCC) cell lines, including SMMC-7721, HepG2, Huh-7, and normal human hepatocytes L-02, were procured from the Cell Bank of the Chinese Academy of Sciences, Shanghai, China. The hepatoma cell lines were cultured in Dulbecco's Modified Eagle Medium (DMEM) supplemented with 10 % fetal bovine serum (FBS) and 1 % penicillin-streptomycin, in a humidified incubator maintained at 37 °C with 5 % CO₂. Conversely, the L-02 cell lines were grown in RPMI Medium 1640.

2.9. qRT-PCR

Cells were harvested for RNA extraction once they occupied approximately 80%–90 % of a 10 cm culture dish. Total RNA was extracted using TRIzol reagents according to the standard protocol. Subsequently, cDNA was synthesized using reverse transcription kits, and the mRNA expression levels were quantified via qPCR assays. GAPDH (glyceraldehyde-3-phosphate dehydrogenase) served as the internal reference for mRNA, and expression levels were calculated using the 2- $\Delta\Delta$ Ct method. The primers for SOX4, AKR1B10, MAGEC2, CYP2C9, S100A11, and MAGEA6, obtained from Sangon Biotech, are detailed in [Supplemental Table S2](#). Additionally, protein expression levels of the six key necroptosis-related genes were examined using the Human Protein Atlas (HPA) online platform.

2.10. Western blot analysis

In 10 % polyacrylamide gels, whole cell proteins were electrophoresed under decreasing conditions. For 1 h, the electrophoresis was performed in MOPS buffer at 180 V. The membrane was blocked in 5 % nonfat dry milk and then incubated with an antibody (Abcam, Cambridge, UK) at a dilution of 1:1000 for a whole night at 4 °C. Using an ECL western blotting kit (Amersham Biosciences, Little Chalfont, UK) and following the manufacturer's instructions, all band intensities were assessed. Image-J software was then used to examine the data.

2.11. Colony assay

One million five hundred cells per six-well plate were planted with cells. After the cells were combined, they were cultivated in culture media with 10 % FBS and L-15 for ten days. The following standards were taken into account when assessing the outcomes: Colonies were defined as groups of at least thirty cells.

2.12. Cell viability assays

2000 cells per well of 96-well plates were used for cell seeding. The Cell Counting Kit-8 assay (CCK-8, Dojindo, Japan) was utilized to detect cell viability in compliance with the manufacturer's protocol. Using an automatic microplate reader (BioTek, Winooski, VT, USA), the absorbance at 450 nm was determined. For seven days in a row, measurements were taken every 24 h.

2.13. Cell migration assays

In the migration assay, 1.5×10^5 cells were introduced to 200 μ l serum-free DMEM in the upper chamber of a Transwell plate (Corning, NY, USA), and 700 μ l DMEM with 20 % serum was added to the lower chamber. Following a 24-h incubation period at 37 °C, the Transwell chamber was taken out, cleaned once using PBS, and then fixed for 30 min using a methanol:acetone ratio of 1:1. It was then stained for 30 min using 0.5 % crystal violet. After carefully wiping away the cells on the upper side of the filter, the chamber was washed with PBS. Using ImageJ, the relative cell density was calculated.

2.14. Statistical analysis

Univariate and multivariate analyses determined the prognostic marker genes. Analyses between the two groups were performed using the Wilcoxon test, and a one-way ANOVA test was used to compare three or more groups. All statistical analyses were performed using R version 4.1.3 (R Core Team) and GraphPad Prism version 8.3 (GraphPad Software, San Diego, CA, USA). The cutoff for significance was chosen at $P < 0.05$.

3. Results

3.1. Identified the necroptosis-related genes by using scRNA

A total of 55341 single cells fulfilled the quality control (QC) described in the materials and methods, including 26660 cells derived

from cancer tissue and 28681 cells derived from peri-tumor samples. These cells were organized into 43 clusters and annotated into 13 main cell types (Fig. 1A). Then we used 25 Necroptosis genes (Supplemental Table S1) and the function AddModuleScore by the Seurat package to annotate score of the necroptosis for the each single cell of HCC. Fig. 1B showed the score of the necroptosis in the distribution of scRNA data. We also listed the expression of each necroptosis gene in each cell type (Fig. 1C). The necroptosis score in the epithelial and endothelial cells were lower than other cell types (Fig. 1D). When apoptosis is suppressed, a regulated cell death called necroptosis causes inflammation and acts as a backup defense mechanism [27]. Hence, we proposed that these hepatoma cells can

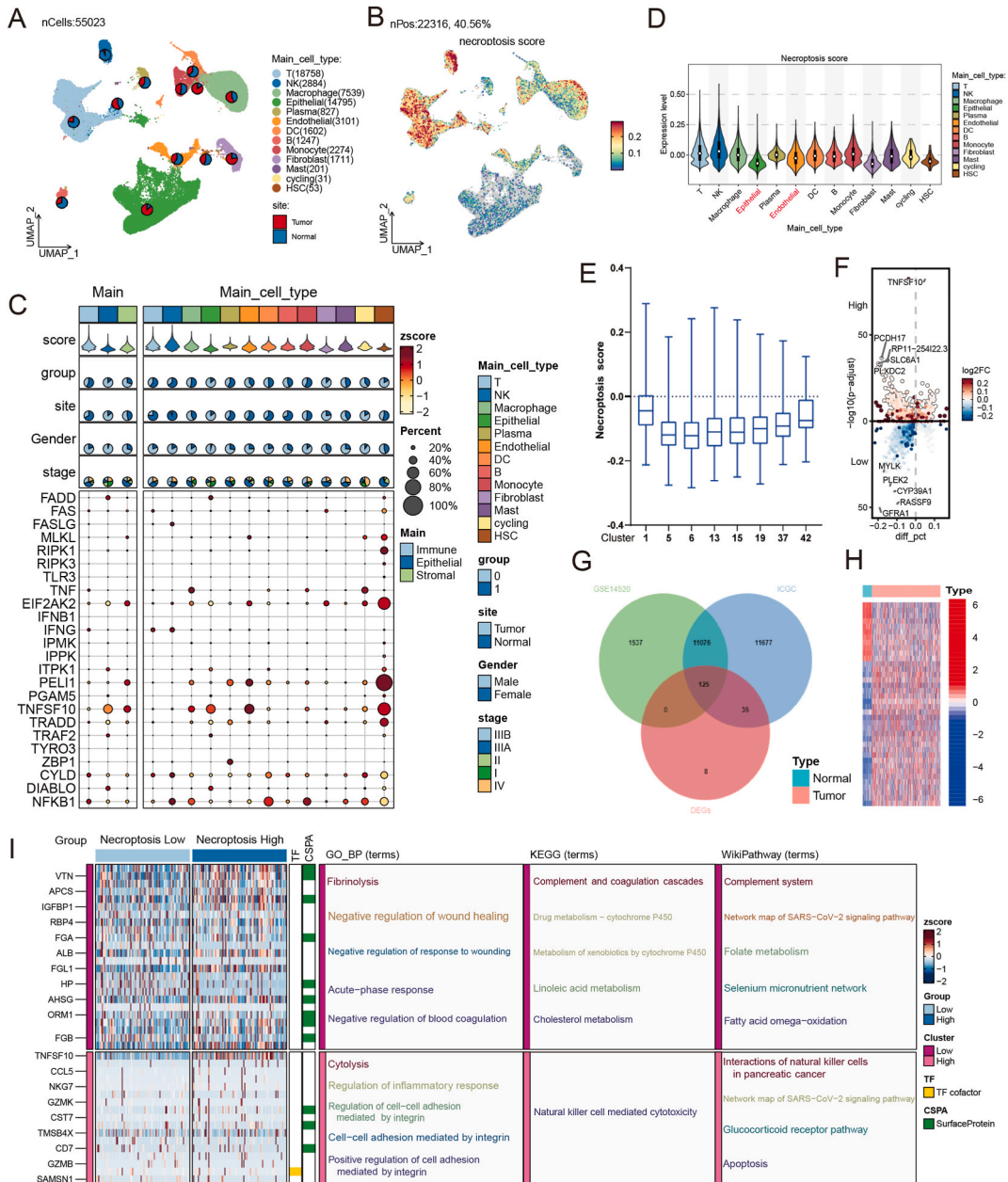


Fig. 1. Analysis of necroptosis-related genes in HCC using single-cell and bulk RNA sequencing data. (A) Distribution of 55,023 cells across 13 cell types in the HCC single-cell RNA (scRNA) dataset. (B) Assessment of necroptosis scores in single-cell RNA data using the AddModuleScore method. (C) Boxplot illustrating variations in necroptosis scores across 13 cell types. (D) Expression profiles of necroptosis genes in the scRNA dataset. (E) Necroptosis score expression in various cancer cell clusters from the scRNA dataset. (F) Differential gene expression between cluster 1 and other clusters in cancer cells. (G) Venn diagram (VennPlot) showing the overlap of 168 DEGs among scRNA DEGs, ICGC-LIHC, and GEO14520 datasets. (H) Expression of 125 DEGs between normal and tumor samples in the TCGA-LIHC cohort. (I) Gene Ontology Biological Process (GO-BP), Kyoto Encyclopedia of Genes and Genomes (KEGG), and WikiPathways analysis for the 125 DEGs, comparing high and low necroptosis-related scores.

promote tumorigenesis and progression by hindering necroptosis [28]. Among these cell lineages, the clusters 1,5,6,13,15,19,37,42 which annotated as hepatoma cells were remained to further analysis. Necroptosis scores of cluster 1 hepatoma cells were low (Fig. 1E). To confirm the genes associated to necroptosis in HCC, the DEGs between hepatoma cells from cluster 1 and other clusters were obtained using the FindAllMarkers function. We obtained 168 Necroptosis-related DEGs by scRNA-seq analysis in HCC (Fig. 1F and Supplemental Table S3). Then, the intersection of 168 DGEs with sequenced genes among multi datasets, 125 genes were all expressed in the ICGC-LIHC and ICGC-LIHC datasets(Fig. 1G). Among them, 38 DEGs were discovered to have significantly different expression values between tumor and normal samples in the TCGA LIHC cohort (Fig. 1H). Using SCP function and GO function

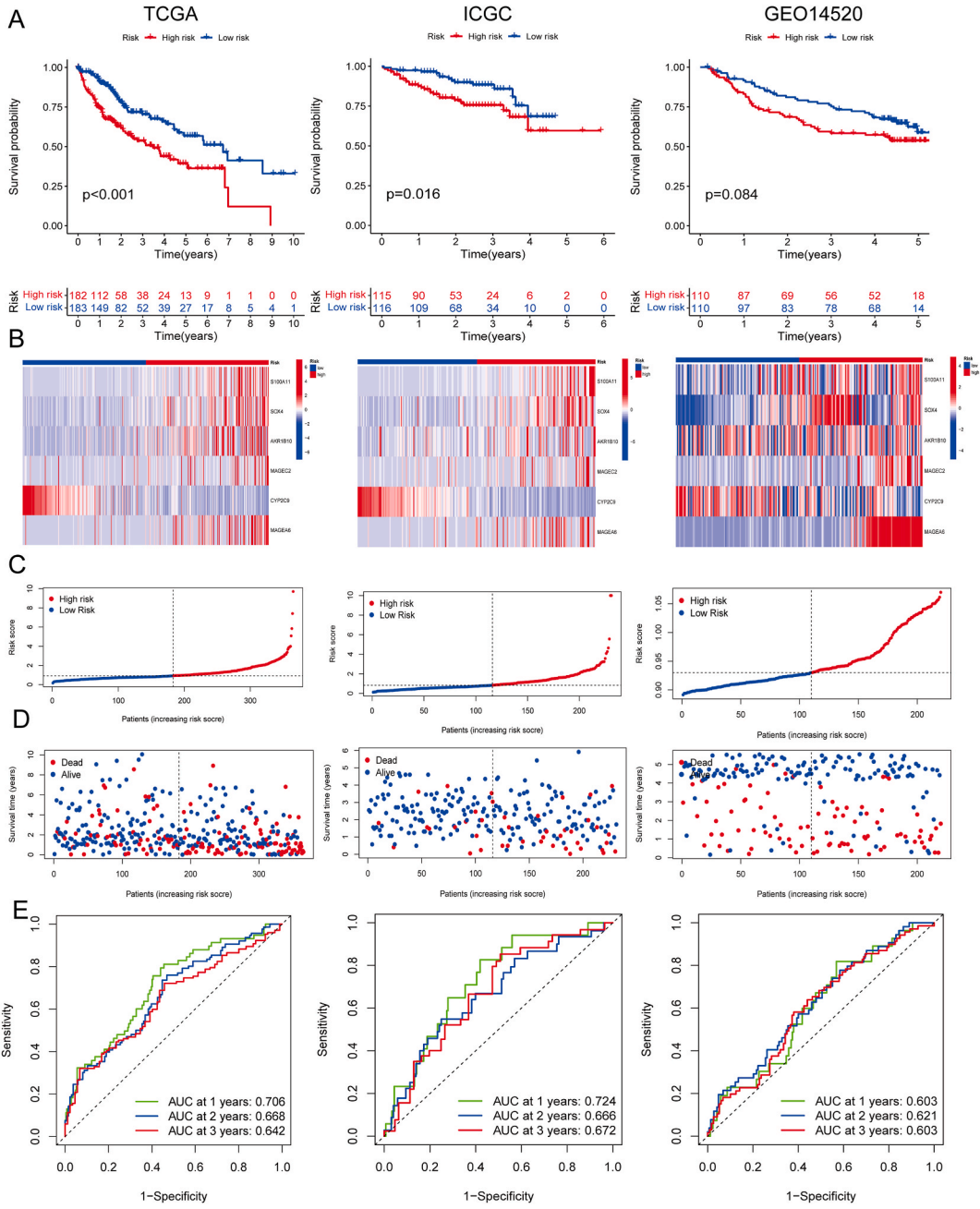


Fig. 2. Evaluation of survival, risk scores, and predictive accuracy in the necroptosis-related model for HCC patients. (A) Kaplan-Meier (K-M) curves for overall survival (OS) comparing high-risk and low-risk groups across TCGA, ICGC, and GSE14520 datasets. (B) Expression patterns of the six genes in the model across high- and low-risk groups. (C) Classification of HCC patients into high- and low-risk categories based on median risk score. (D) Distribution of survival status and risk scores of HCC patients in TCGA, ICGC, and GSE14520 datasets. (E) Receiver Operating Characteristic (ROC) curves of the Necroptosis-Related Prognostic Model for 1-, 3-, and 5-year OS predictions.

analysis, we found that these DEGs were associated with several function and KEGG pathways involved in necroptosis, such as fibrinolysis, response to negative regulation of wound healing, acute-phase response, negative regulation of blood coagulation, Complement and coagulation cascades, cholesterol metabolism and linoleic acid metabolism. etc(Fig. 11).

3.2. Establishment and Validation of necroptosis-related modeling signature

We identified 12 DEGs connected to prognosis in HCC using univariate Cox regression analysis, with 11 unfavored and 1 favored gene (Supplemental Table S4). These prognosis-related DEGs were incorporated in the subsequent multivariate Cox regression algorithm to improve the model’s independent predicting capacity. Finally, six DEGs were integrated as necroptosis-related modeling genes (NRMGs) to generate the necroptosis-Related modeling Score (NRMG-Score). The following formula was then utilized to determine the risk-score: $Riskscore = (0.0007 * S100A11) + (0.0152 * SOX4) + (0.0005 * AKR1B10) + (0.0089 * MAGEC2) + (-0.0019 * CYP2C9) + (0.01829 * MAGEA6)$.

In the TCGA cohort (Training dataset), patients in the high-risk subset possessed a poor outcome, which was further confirmed by ICGC dataset (Fig. 2A). Additionally, we also observed high-risk patients in GSE14520 cohort possessed a negative prognostic tendency (p = 0.08). Every patient in the training and test subsets had their risk-score determined, and the median risk-score value was applied to categorize patients into high- and low-risk subsets (Fig. 2B and C). Meanwhile, the death rate for the high-risk subset was also significantly greater than for the low-risk subgroup (Fig. 2D). Furthermore, our ROC analysis suggested the risk model performed with good predictive accuracy, with area under curve (AUC) values of 0.706 in the one-year ROC curve, 0.668 in the two-year ROC curve, and 0.642 in the three-year ROC curve in TCGA sets. AUC values of one, two, and three-year ROC curves in ICGC sets were 0.724, 0.666, and 0.672, respectively (Fig. 2E).

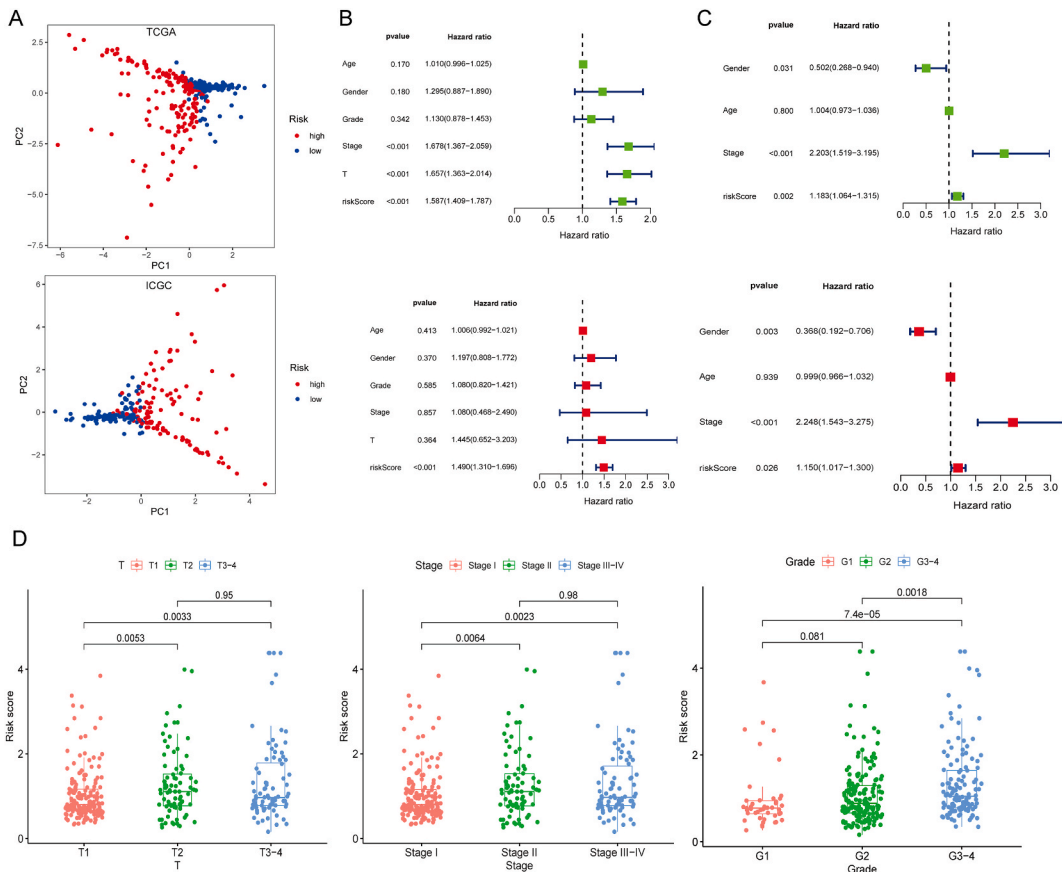


Fig. 3. Association of necroptosis-related model gene (NRMG) scores with Clinicopathological Features in HCC. (A) Principal Component Analysis (PCA) illustrating distinct distribution of patients in different risk groups within TCGA and ICGC datasets. (B) and (C) Univariate (upper) and multivariate (bottom) analyses indicating the risk score as an independent prognostic factor in comparison to other clinical characteristics in both TCGA (B) and ICGC datasets. (D) Variation in NRMG scores across different TNM stages and grades in the TCGA cohort.

3.3. NRMGs score was an independent clinical risk factor

PCA plot displayed high-risk patients could be distinguished from low-risk patients using our NRMG-SCORE predict model (Fig. 3A). Furthermore, univariate and multivariate Cox regression algorithms revealed the risk-score was a prognostic indicator independent of certain other clinical characteristics in both TCGA and ICGC sets (Fig. 3B and C). The risk-score is correlated with tumor size, stage, and tumor grade (Fig. 3D), and patients with high tumor grade and stage owned higher risk-score ($P < 0.05$).

3.4. Immune infiltration for NRMG-SCORE in bulk sequence RNA level

We calculated the immune cell infiltrates for high- and low-risk subsets to examine the potential roles of NRMG-SCORE in tumorigenesis and development, including SOX4, AKR1B10, MAGEC2, CTP2C9, S100A11, and MAGEA6. Interestingly, individuals in the high-risk subset exhibited higher immune cell infiltrates. Treg cells, Follicular helper T cells, Th2 cells, and macrophages were

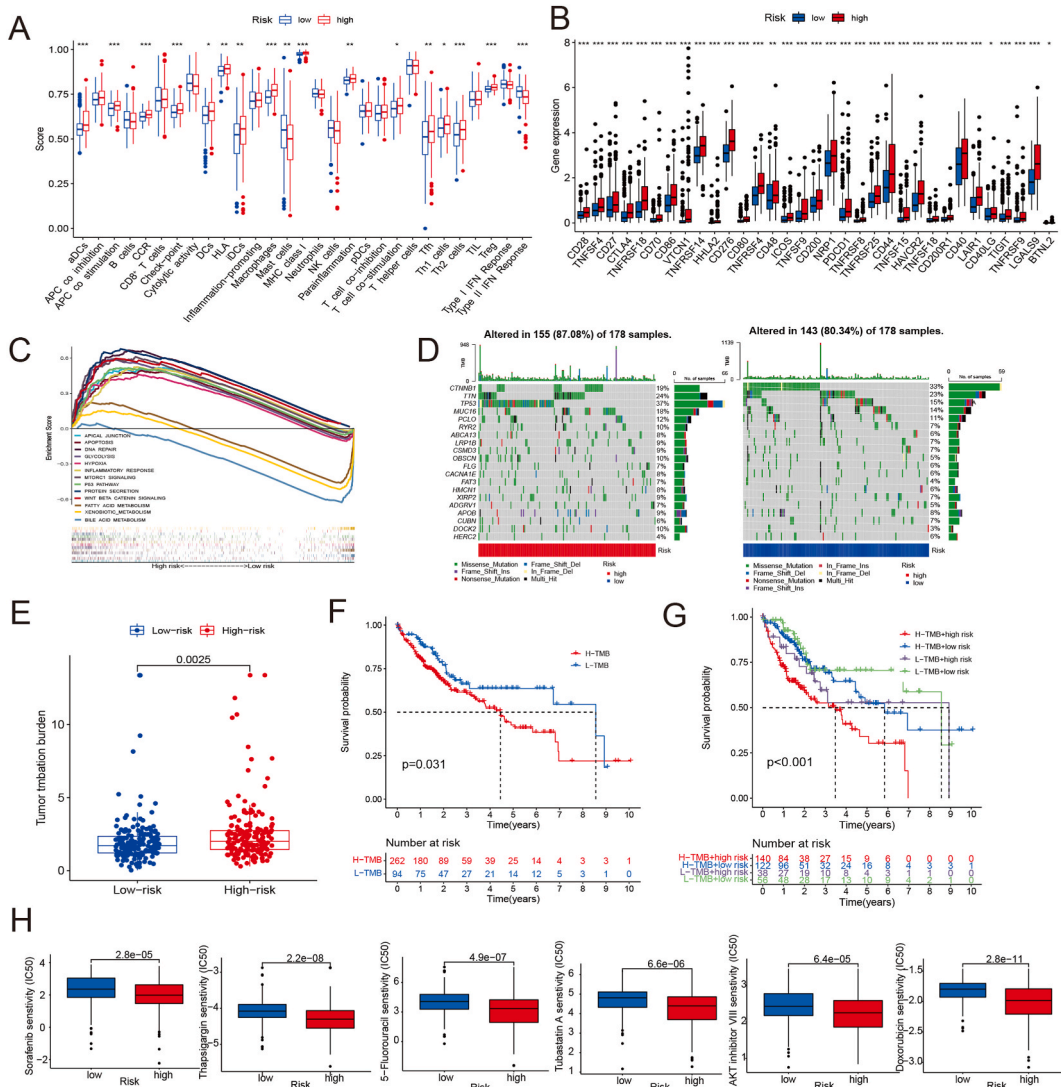


Fig. 4. Analysis of immune infiltration, Functional enrichment, and drug sensitivity in Relation to necroptosis-related model gene (NRMG) scores. (A) Bar plot depicting differences in immune cell infiltration between high-risk and low-risk groups. (B) Comparative expression levels of immune checkpoints in high- and low-risk groups. (C) Gene Set Enrichment Analysis (GSEA) results highlighting enrichment of WNT beta-catenin signaling, P53 pathways, glycolysis pathways, and hypoxia in the high-risk group. (D) Waterfall plot showing somatic mutation characteristics in patients with high and low risk scores. Each column represents an individual patient, with the upper bar plot indicating Tumor Mutation Burden (TMB), and the right-hand numbers showing mutation frequency in each gene. (E) Correlation between risk score and TMB. (F) Kaplan-Meier curve for overall survival in high- and low-TMB groups. (G) Kaplan-Meier curve evaluating patient overall survival based on a combination of risk score and TMB. (H) Comparison of estimated IC50 values for various drugs between high-risk and low-risk groups.

enriched in the high-risk subset (Fig. 4A). However, when we calculated the degree of immune checkpoint expression, we found that most of these genes, including PDCD1(programmed cell death protein 1) and CTLA4, were significantly overexpressed in high-risk subset (Fig. 4B). We proposed although patients in the high-risk subset possessed higher levels of immune infiltration, the high expression of immune checkpoints resulted in a weak anti-tumor state. These patients may gain high response rates during immunotherapy. Our necroptosis-related risk model might offer a fresh way to forecast the effectiveness of immunotherapy. The most

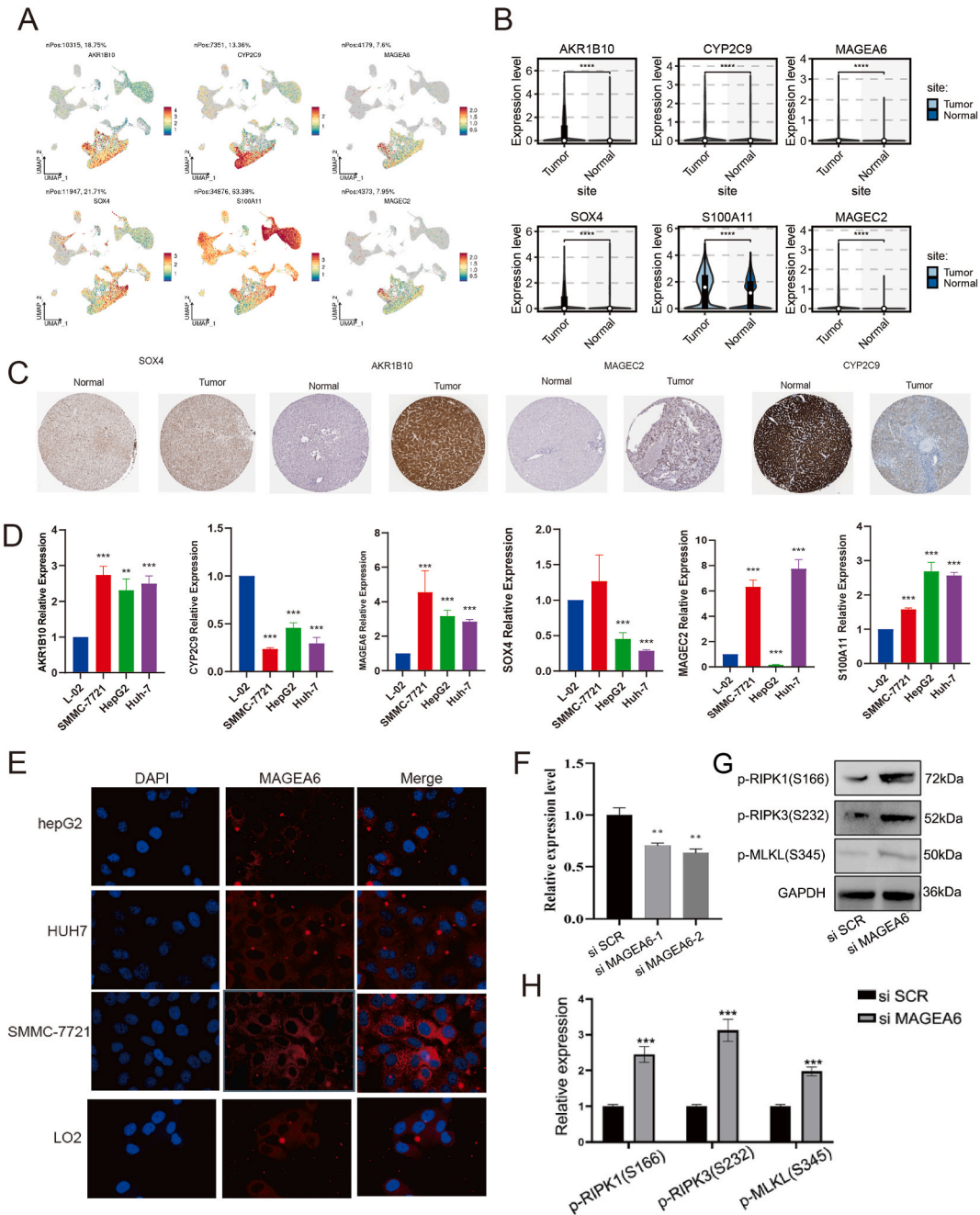


Fig. 5. Elucidating the Central role of MAGEA6 in HCC based on necroptosis-related model gene (NRMG) score. (A) UMAP plot showing expression levels of model genes across different cell types. (B) Boxplot comparing expression of six key genes between tumor and normal tissues in single-cell RNA (scRNA) data. (C) Immunohistochemical images from the Human Protein Atlas (HPA) dataset illustrating expression of the six model genes in tumor and adjacent non-tumor tissues.(D) Quantitative real-time PCR (qRT-PCR) analysis revealing mRNA levels of six NRMGs in hepatoma and normal hepatocyte cell lines. (E) Immunofluorescence assays indicating highest fluorescence intensity in SMMC-7721 cells. (F) qPCR results demonstrating significant inhibition of MAGEA6 expression in SMMC-7721 cells by Si-MAGEA6-1 and Si-MAGEA6-2. (G) Elevated expression levels of necroptosis-related proteins (p-RIPK1, p-RIPK3, and p-MLKL) following MAGEA6 knockdown.

important component of TME, tumor immune microenvironment (TIME), is essential for the tumorigenesis and treatment resistance [29].

3.5. Function enrichment analysis for NRMG-score in bulk sequence RNA level

GSEA results revealed that WNT beta-catenin signaling, P53 pathways, glycolysis pathways, and hypoxia were enriched in the high-risk subset (Fig. 4C). Inadequate blood supply or hypoxia is a typical microenvironmental characteristic of almost all solid tumors due to their rapid and uncontrolled proliferation. Hypoxic regions promote abnormal angiogenesis [30,31], adhesion proliferation, and inflammation [32]. GO analysis displayed immune-related pathways, like leukocyte-mediated immunity, T cell activation, leukocyte migration, and cytokine-mediated signaling pathway, were significantly enriched in high-risk subset patients (Fig. S1). Moreover, KEGG analysis uncovered that glycolysis/gluconeogenesis, IL-17 signaling pathway, ECM-receptor interaction, and cytokine-cytokine receptor interaction were up-regulated in the low-risk subset (Fig. S2).

3.6. The mutation Landscape in Necroptosis-Related Prognostic Model

According to the GSEA results, the P53 pathway was concentrated in the high-risk subset. We then estimated the somatic mutation rate in the two risk subsets. The P53 mutation rate was 37 % in 178 high-risk subset patients, which was obviously greater than the 15 % P53 mutation rate in the low-risk subset patients (Fig. 4D). TP53 is a tumor suppressor gene mutated in more than half of all human cancers. Tumors with P53 mutations progress faster, respond poorly to anti-cancer therapy, and have a worse outcome [33]. P53 mutations are more common in high-risk patients, implying that NRMGs are involved in the P53 pathway. The TMB values were compared between the high- and low-risk subsets, and it was obvious that patients in the high-risk subset had significantly higher TMB than those in the low-risk subset ($p = 0.0025$) (Fig. 4E). Patients with cancer typically have a poor prognosis if their TMB is high. In our research, the HCC patients' outcome with a high TMB was also worse (Fig. 4F). We combined TMB and NRMGs for survival analysis due to their synergistic effect on prognosis. According to our findings, patients with a high-risk score and a high TMB owned the worst prognosis (Fig. 4G). These analyses suggested that the combination of NRMGs and TMB could further refine the prognosis prediction of patients.

3.7. Analyses of drug sensitivity and Cell Localization of six modeling genes

We calculated the concentration causing a 50 % reduction growth (IC50) of drugs to determine which drugs have significantly different sensitivities between high- and low-risk subsets using the pRRophetic R package to integrate prognostic models with clinical practice. The high-risk subset patients possessed higher sensitivity to Sorafenib, Thapsigargin, Tubastatin, Ruxolitinib, Rapamycin, 5-Fluorouracil, AKT inhibitor VIII, Doxorubicin, Imatinib, and Lisitinib (Fig. 4H).

3.8. Potential necroptosis regulated model genes promote the progress of HCC

We used single-cell sequencing to determine the expression levels of the modeling genes in each cell type. As seen in Fig. 5A and B, SOX4, AKR1B10, MAGEC2, CTP2C9, and MAGEA6 were primarily expressed in hepatoma cells and hepatocytes, while S100A11 was detected in hepatoma cells, hepatocytes, immune cells, fibroblasts, and endothelial cells. We also detected the protein expression values of six modeling genes using the HPA database. HCC tumor tissue exhibited overexpression of SOX4, AKR1B10, MAGEC2, and CTP2C9 relative to normal tissue (Fig. 5C). Simultaneously, we compared the mRNA expression levels of L-02 cell lines and three HCC cell lines. MAGEA6, AKR1B10, and S100A11 had higher mRNA expression levels in SMMC-7721, HepG2, and Huh-7, than in L-02. The mRNA expression of MAGEC2 was upregulated in SMMC-7721 and Huh-7 and decreased in HepG2. In contrast to L-02, CTP2C9 and SOX4 levels were lower in HCC cell lines (Fig. 5D).

In order to explore the expression of MAGEA6 in HCC cells, we conducted immunofluorescence experiments, and the results showed that the fluorescence intensity was the highest in SMMC-7721 cells (Fig. 5E), which proved that MAGEA6 was the highest in SMMC-7721 cells, and we selected SMMC-7721 cells for further experiments. To gain insights into the function of MAGEA6, we characterized the oncogenic phenotypes in SMMC-7721 cells with MAGEA6 silencing (Si-MAGEA6-1 and Si-MAGEA6-2). The qPCR results showed that Si-MAGEA6-1 and Si-MAGEA6-2 could significantly inhibit MAGEA6 expression in SMMC-7721 cells (Fig. 5F), and we chosen Si-MAGEA6-1 for cell function experiments. Next, to figure out the effect of si MAGEA6 on cell necroptosis, Western blot assay was performed. As shown in Fig. 5C, the expression levels of cell necroptosis-related proteins (p-RIPK1, p-RIPK3 and p-MLKL) were up-regulated after MAGEA6 knockdown.

3.9. The biological role of MAGEA6 in SMMC-7721 cell lines

We investigated the role of the MAGEA6 in the proliferation of HCC cells by colony-formation, CCK8 and immunofluorescence assay. To assess the influence of the MAGEA6 on cell death and apoptosis, a LDH, PI and flow cytometry assays was used to detect. colony-formation (Fig. 6A), CCK8 (Fig. 6B) and immunofluorescence (Fig. 6C) assay revealed that knockdown of MAGEA6 inhibited the proliferation of HCC cells. Additionally, knockdown of MAGEA6 significantly promoted HCC cell death and apoptosis (Fig. 6D–F). Fig. 6 showed the transwell assays revealed that knockdown of circCCDC134 impaired the migration of HCC cells.

4. Discussion

Human cells destroy themselves to preserve biological equilibrium and shield the body from pathogens, a process known as regulated cell death (RCD). Moreover, RCD is classified as apoptotic and non-apoptotic forms [34]. For more than three decades, clinical researchers have been working on therapies that promote the effective elimination of cancer cells via apoptosis. However, tumor cells can avoid apoptosis, resulting in treatment resistance and cancer relapse [35]. Researchers are focusing on alternative cancer cell death processes, including autophagy, necroptosis, pyroptosis, paraptosis, and ferroptosis, and converting apoptosis to these RCDs has the potential to overcome apoptosis resistance. Contradictory findings from research on necroptosis' role in cancer suggest that necroptosis has distinct impacts at different stages of cancer cell growth and metastasis [12,36,37]. Tumor cells and non-tumor cells interact to generate a complicated TME. Researchers hope to restrict tumor growth by inducing necroptosis in malignant cells. However, necroptosis would change the tumor microenvironment to a certain degree, and the impact on TME is uncertain. In contrast, necroptosis may prevent tumors from anti-cancer immune responses by promoting an immunosuppressive environment [13,38]. Contrarily, necroptosis may cause strong anti-tumor immunity, and its processes and ICLs may synergistically improve anti-tumor activity, even in cancer types resistant to ICLs [39]. Over the last decade, targeted therapies have paved the path for personalized precision medicine. Targeted therapy like Sorafenib, Lenvatinib, and ICLs, however, may only be effective for a small percentage of HCC patients. Furthermore, drug-related side effects and resistance continue to be a concern. Therefore, exploring the mechanisms of necroptosis in HCC and their impact on TIME will pave the way for ICI-based combination therapy. Meanwhile, exploring the necrosis-related genes may lead to new therapeutic targets or enhance the prediction of HCC prognosis. In this work, we explored genes related to necroptosis using single-cell sequencing to see if they could predict HCC prognosis. After univariate and multivariate Cox regression algorithms, a necroptosis-related genes risk model comprising six genes was established using the TCGA database and verified in the ICGC database. Patients in the high-risk group possessed a poor outcome, and the risk-score was a prognostic indicator that could be used independently of other clinical traits. Additionally, the high-risk subset patients exhibited increased levels of immune infiltration, and the high level of immune checkpoints resulted in a weak anti-tumor state. Hypoxia, glycolysis, and P53 pathway were enriched in the high-risk subset; the rate of P53 somatic mutations was also considerably greater. Furthermore, expression values of six modeling genes differed significantly between normal hepatocyte and hepatoma cell lines.

We used HCC single-cell sequencing data for the first time to assess the necroptosis score for each cell type. Hepatoma cells exhibited the lowest necroptosis score when compared with other cell types, revealing they may have a defense mechanism against

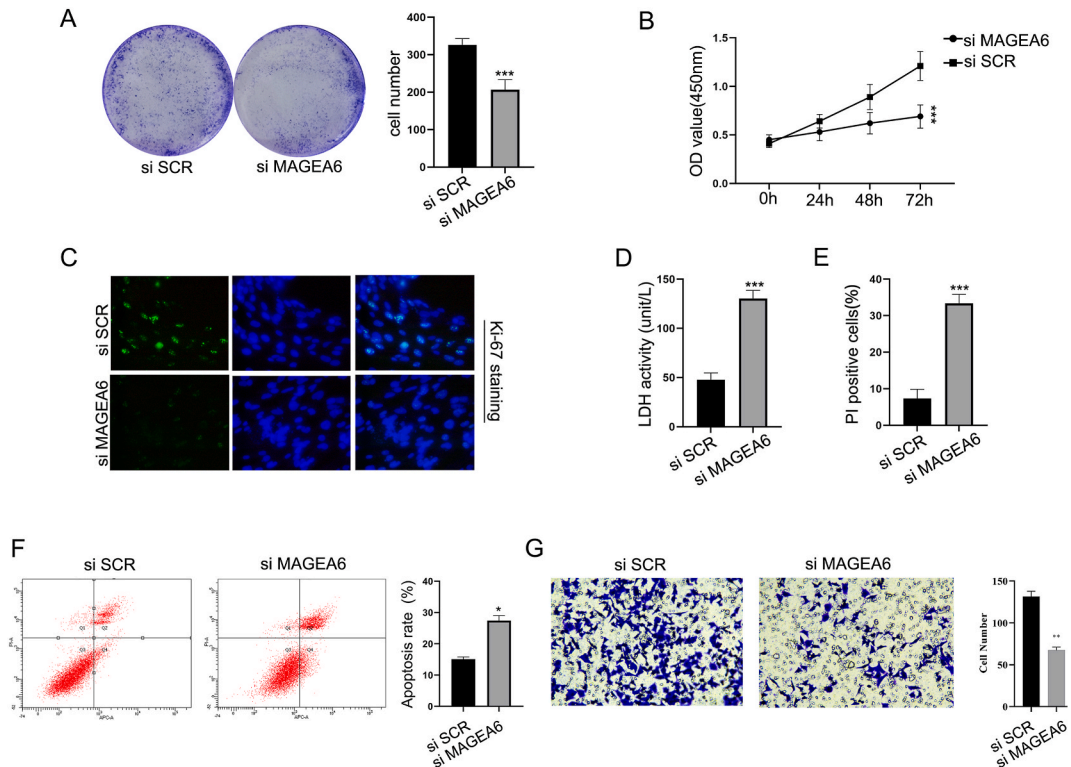


Fig. 6. Investigating the impact of MAGEA6 on hepatocellular carcinoma (HCC) Cell proliferation. (A) Colony formation assay results. (B) Cell Counting Kit-8 (CCK8) assay outcomes. (C) Findings from immunofluorescence assays. (D-F) Results indicating that knockdown of MAGEA6 notably enhances cell death and apoptosis in HCC cells. (G) Transwell assays demonstrating reduced cell migration following the knockdown of circCCDC134 in HCC cells.

necroptosis. Several studies have found that inducing necroptosis in hepatoma cell lines can inhibit the growth of tumor cells. Xiang et al. identified shikonin, a necroptosis inducer, may be more effective than apoptosis inducers in eliminating HCC cells with high Cx32 expression [40]. According to recent research, excessive Sorbitol dehydrogenase in HCC cells hinders the growth of tumor cells by promoting necroptosis [41]. Therefore, stimulating necroptosis to kill hepatoma cells is a promising therapeutic approach. However, the downstream mechanisms of necroptosis have not been fully studied. We further explored necroptosis-related genes using single-cell sequencing techniques to find more targets associated with necroptosis. Using single-cell data, 168 DEGs associated with necroptosis were identified. They were enriched in response to a toxic substance, acute inflammatory response, and neutrophil degranulation, all of which were involved in necroptosis. Based on these DGEs, we successfully constructed a prognostic model that precisely estimates the difference in prognosis between HCC patients in the high and low-risk cohorts. ROC analysis indicated the gene signature worked well in predictive accuracy, with AUC values of 0.706 in the one-year ROC curve, 0.668 in the two-year ROC curve, and 0.642 in the three-year ROC curve in TCGA sets. The AUC value of the one, two, and three-year ROC curves in ICGC sets were 0.724, 0.666, and 0.672, respectively. Besides, our risk model was a prognostic indicator independent of other clinical characteristics, such as tumor size, stage, and grade. Therefore, our CCGs prognostic model may be employed to evaluate the outcome and survival time of HCC patients.

Six NRMGs have been studied in HCC, including S100A11, MAGEC2, MAGEA6, CYP2C9, SOX4, and AKR1B10. During necroptosis, a large quantities of damage associated molecular patterns (DAMPs), including S100 protein family members, are released [42]. A calcium-binding protein called S100 is connected to numerous pathological and disease processes, including inflammation and carcinogenesis. Numerous members of the S100 protein family appear to be crucial in the emergence of hepatic steatosis, non-alcoholic steatohepatitis (NASH), and HCC [43]. High-grade HCC and poor prognosis are highly correlated with overexpression of S100A11, which promotes inflammation/fibrosis and early dysregulated steatosis [44]. In intrahepatic cholangiocarcinoma, P38/MAPK signaling pathway activation, colony formation, and proliferation of RBE and HCCC9810 cells were all dramatically reduced when S100A11 was silenced *In vitro*. *In vivo*, tumor growth was also prevented [45]. MAGEA6 and MAGEC2 are members of the MAGE family, and the MAGE gene originally received attention among oncologists because of its strong tumor antigenic characteristics in melanoma. MAGE genes are found to be dysregulated in a variety of tumors [46]. miR-448 promotes the AMPK signaling pathway through the downregulation of MAGEA6, thereby inhibiting stemness maintenance and proliferation of HCC stem cells [47]. Similarly, MAGEC2 has been associated with metabolic reprogramming in HCC [48]. The expression of CYP2C9, one of the most prevalent and significant xenobiotic metabolizing enzymes, is downregulated in HCC. CYP2C9 is involved in developing hepatocarcinogenesis and regulates cell proliferation, apoptosis, differentiation, and homeostasis [49]. SOX4 activates CXCL12 to induce endothelial cell chemotaxis, angiogenesis, and tumor growth [50]. Meanwhile, targeting SOX4 can inhibit cell proliferation and migration [51]. Higher levels of AKR1B10 expression are linked to a worse long-term prognosis, making it a viable biomarker for HCC. According to multiple experimental studies, silencing AKR1B10 causes cell death and inhibits tumor development and spread [52]. Meanwhile, the down-regulated expression of AKR1B10 in NK cells promotes glycolysis while inhibiting migration, invasion, and metastasis of hepatoma cells [53]. In this research, we explored the mRNA value of six NRMGs in hepatoma cells and hepatocyte cell lines using qrt-PCR. The six modeling genes expression significantly differed between normal hepatocyte and hepatoma cell lines, indicating they might be a potential target for treatment.

Effective anti-tumor immunity can fight cancer cells and boost the prognosis of HCC patients. Cancer cells suppressed the immune cell's function to promote immune escape by creating a hypoxic and hyper-lactic environment and reprogramming immune cells [54]. Therefore, stimulating anti-tumor immunity is a promising therapeutic approach, and ICIs are developed based on this theory. Currently, researchers are investigating tumor immunity and looking for fresh targets to activate anti-tumor immune responses. Individual in the high-risk subset in our necroptosis-related prognostic signature exhibit greater immune cell infiltration. Meanwhile, most immune checkpoints were over-expressed in the high-risk subset, and immune checkpoints activation can suppress T lymphocyte function and hence the auto-immune response. Immune checkpoint expression has become a predictor of immunotherapy effectiveness, with higher expression resulting in higher response rates. Hence, the different risk-scores based on the necroptosis-related risk model might serve as a promising indicator for immunotherapy strategy. In addition, TMB was noticeably higher in the high-risk subset, and patients in this subset owned a poor prognosis. TMB is a commonly used immunotherapy response biomarker in clinical practice, with high TMB levels indicating a high rate of immunotherapy response. This is consistent with our previous inference that patients in the high-risk subset are probably receiving benefits from ICIs. Finally, compared to the low-risk subset, the high-risk subset exhibited a much greater rate of P53 mutations, with most of these mutations being missense mutations. TP53 is a tumor suppressor gene, suggesting that NRMGs are involved in the P53-related pathway, which was also confirmed by GSEA analysis. Functional analysis suggested that NRMGs are involved in immune-related pathways including leukocyte-mediated immunity, T-cell activation, leukocyte migration, and cytokine-mediated signaling pathways. DAMPs, as well as inflammatory cytokines and chemokines, can be released in large quantities during necroptosis, resulting in an inflammatory response [55,56]. According to Zhang et al., ICI resistance in melanoma could be overcome by inducing ZBP1-dependent necroptosis in cancer-associated fibroblasts [57]. Overall, necroptosis and its immunobiology cannot be generalized or applied to a complicated pathology like cancer in a "black and white" way. To effectively utilize necroptosis as a therapeutic target, the specific chemical mechanisms and signaling systems involved must be understood.

In sum up, a six NRMGs risk model was developed for the independent prediction of the prognosis of HCC patients. The riskscores could be employed as an indicator for immunotherapy.

Funding

This work was supported by the National Natural Science Foundation project of China (82372194), Tianjin Health Science and Technology Project of China (TJWJ2023MS012).

Data availability

The data involved in our work are available in the TCGA (<https://gdc.cancer.gov/cancer-genome-atlas-tcga>), ICGC (<https://dcc.icgc.org/>), and GEO (<https://www.ncbi.nlm.nih.gov/geo/>).

CRediT authorship contribution statement

Youcheng Zhang: Writing – original draft, Methodology, Data curation. **Dapeng Chen:** Writing – original draft, Methodology. **Bing Ang:** Data curation. **Xiyue Deng:** Software. **Bing Li:** Validation. **Yi Bai:** Software. **Yamin Zhang:** Writing – review & editing, Methodology, Investigation.

Declaration of competing interest

The authors declare that they have no known competing financial interests or personal relationships that could have appeared to influence the work reported in this paper.

Appendix A. Supplementary data

Supplementary data to this article can be found online at <https://doi.org/10.1016/j.heliyon.2024.e37711>.

References

- [1] H. Sung, J. Ferlay, R.L. Siegel, et al., Global cancer statistics 2020: GLOBOCAN estimates of incidence and mortality worldwide for 36 cancers in 185 countries, *CA Cancer J Clin* 71 (3) (2021) 209–249.
- [2] K.A. McGlynn, J.L. Petrick, H.B. El-Serag, Epidemiology of hepatocellular carcinoma, *Hepatology* 73 (Suppl 1) (2021) 4–13.
- [3] D. Anwanwan, S.K. Singh, S. Singh, et al., Challenges in liver cancer and possible treatment approaches, *Biochim. Biophys. Acta Rev. Canc* 1873 (2020) 188314.
- [4] F. Martínez-Jiménez, F. Muiños, I. Sentís, et al., A compendium of mutational cancer driver genes, *Nat. Rev. Cancer* 20 (2020) 555–572.
- [5] M. Pinter, R.K. Jain, D.G. Duda, The current landscape of immune checkpoint blockade in hepatocellular carcinoma: a review, *JAMA Oncol.* 7 (2021) 113–123.
- [6] A.L. Cheng, C. Hsu, S.L. Chan, et al., Challenges of combination therapy with immune checkpoint inhibitors for hepatocellular carcinoma, *J. Hepatol.* 72 (2020) 307–319.
- [7] A. Sharma, L.H. Boise, M. Shanmugam, Cancer metabolism and the evasion of apoptotic cell death, *Cancers* 11 (2019).
- [8] W. Gao, X. Wang, Y. Zhou, et al., Autophagy, ferroptosis, pyroptosis, and necroptosis in tumor immunotherapy, *Signal Transduct Target Ther* 7 (2022) 196.
- [9] Y. Wang, T.D. Kanneganti, From pyroptosis, apoptosis and necroptosis to PANoptosis: a mechanistic compendium of programmed cell death pathways, *Comput. Struct. Biotechnol. J.* 19 (2021) 4641–4657.
- [10] G. Stoll, Y. Ma, H. Yang, et al., Pro-necrotic molecules impact local immunosurveillance in human breast cancer, *Oncolimmunology* 6 (2017) e1299302.
- [11] X. Feng, Q. Song, A. Yu, et al., Receptor-interacting protein kinase 3 is a predictor of survival and plays a tumor suppressive role in colorectal cancer, *Neoplasma* 62 (2015) 592–601.
- [12] Q. Wang, W. Chen, X. Xu, et al., RIP1 potentiates BPDE-induced transformation in human bronchial epithelial cells through catalase-mediated suppression of excessive reactive oxygen species, *Carcinogenesis* 34 (2013) 2119–2128.
- [13] H.H. Park, H.R. Kim, S.Y. Park, et al., RIPK3 activation induces TRIM28 derepression in cancer cells and enhances the anti-tumor microenvironment, *Mol. Cancer* 20 (2021) 107.
- [14] S. Park, K.J. Hatanpaa, Y. Xie, et al., The receptor interacting protein 1 inhibits p53 induction through NF-kappaB activation and confers a worse prognosis in glioblastoma, *Cancer Res.* 69 (2009) 2809–2816.
- [15] Y. Gong, Z. Fan, G. Luo, et al., The role of necroptosis in cancer biology and therapy, *Mol. Cancer* 18 (2019) 100.
- [16] L. Della Torre, A. Nebbioso, H.G. Stunnenberg, et al., The role of necroptosis: biological relevance and its involvement in cancer, *Cancers* 13 (2021).
- [17] L. Nicolè, T. Sanavia, R. Cappellesso, et al., Necroptosis-driving genes RIPK1, RIPK3 and MLKL-p are associated with intratumoral CD3(+) and CD8(+) T cell density and predict prognosis in hepatocellular carcinoma, *J Immunother Cancer* 10 (2022).
- [18] S. Mohammed, N. Thadathil, R. Selvarani, et al., Necroptosis contributes to chronic inflammation and fibrosis in aging liver, *Aging Cell* 20 (2021) e13512.
- [19] X. Chen, B. Cheng, D. Dai, et al., Heparanase induces necroptosis of microvascular endothelial cells to promote the metastasis of hepatocellular carcinoma, *Cell Death Discov* 7 (2021) 33.
- [20] J. Lu, C. Yu, Q. Bao, et al., Identification and analysis of necroptosis-associated signatures for prognostic and immune microenvironment evaluation in hepatocellular carcinoma, *Front. Immunol.* 13 (2022) 973649.
- [21] Z. Li, J. Fang, S. Chen, et al., A risk model developed based on necroptosis predicts overall survival for hepatocellular carcinoma and identification of possible therapeutic drugs, *Front. Immunol.* 13 (2022) 870264.
- [22] Y. Lu, A. Yang, C. Quan, et al., A single-cell atlas of the multicellular ecosystem of primary and metastatic hepatocellular carcinoma, *Nat. Commun.* 13 (2022) 4594.
- [23] A. Butler, P. Hoffman, P. Smibert, et al., Integrating single-cell transcriptomic data across different conditions, technologies, and species, *Nat. Biotechnol.* 36 (2018) 411–420.
- [24] A. Narayan, B. Berger, H. Cho, Assessing single-cell transcriptomic variability through density-preserving data visualization, *Nat. Biotechnol.* 39 (2021) 765–774.
- [25] J. Yan, P. Wan, S. Choksi, et al., Necroptosis and tumor progression, *Trends Cancer* 8 (2022) 21–27.
- [26] G. Yu, L.G. Wang, Y. Han, et al., clusterProfiler: an R Package for Comparing Biological Themes Among Gene Clusters, vol. 16, *OMICS*, 2012, pp. 284–287.

- [27] A. Negroni, E. Colantoni, S. Cucchiara, et al., Necroptosis in intestinal inflammation and cancer: new concepts and therapeutic perspectives, *Biomolecules* 10 (2020).
- [28] B. Tummers, L. Mari, C.S. Guy, et al., Caspase-8-Dependent inflammatory responses are controlled by its adaptor, FADD, and necroptosis, *Immunity* 52 (2020) 994–1006.e8.
- [29] T. Fu, L.J. Dai, S.Y. Wu, et al., Spatial architecture of the immune microenvironment orchestrates tumor immunity and therapeutic response, *J. Hematol. Oncol.* 14 (2021) 98.
- [30] X. Jing, F. Yang, C. Shao, et al., Role of hypoxia in cancer therapy by regulating the tumor microenvironment, *Mol. Cancer* 18 (2019) 157.
- [31] B. Wang, Q. Zhao, Y. Zhang, et al., Targeting hypoxia in the tumor microenvironment: a potential strategy to improve cancer immunotherapy, *J. Exp. Clin. Cancer Res.* 40 (2021) 24.
- [32] J. Lin, X. Wang, S. Zhai, et al., Hypoxia-induced exosomal circPDK1 promotes pancreatic cancer glycolysis via c-myc activation by modulating miR-628-3p/BPTF axis and degrading BIN1, *J. Hematol. Oncol.* 15 (2022) 128.
- [33] J. Hu, J. Cao, W. Topatana, et al., Targeting mutant p53 for cancer therapy: direct and indirect strategies, *J. Hematol. Oncol.* 14 (2021) 157.
- [34] L. Galluzzi, I. Vitale, S.A. Aaronson, et al., Molecular mechanisms of cell death: recommendations of the nomenclature committee on cell death 2018, *Cell Death Differ.* 25 (2018) 486–541.
- [35] B.A. Carneiro, W.S. El-Deiry, Targeting apoptosis in cancer therapy, *Nat. Rev. Clin. Oncol.* 17 (2020) 395–417.
- [36] U. Höckendorf, M. Yabal, T. Herold, et al., RIPK3 restricts myeloid leukemogenesis by promoting cell death and differentiation of leukemia initiating cells, *Cancer Cell* 30 (2016) 75–91.
- [37] Q. Han, Y. Ma, H. Wang, et al., Resibufogenin suppresses colorectal cancer growth and metastasis through RIP3-mediated necroptosis, *J. Transl. Med.* 16 (2018) 201.
- [38] S.T. Workenhe, A. Nguyen, D. Bakhshinyan, et al., De novo necroptosis creates an inflammatory environment mediating tumor susceptibility to immune checkpoint inhibitors, *Commun. Biol.* 3 (2020) 645.
- [39] L. Seifert, G. Werba, S. Tiwari, et al., The necrosome promotes pancreatic oncogenesis via CXCL1 and Mincle-induced immune suppression, *Nature* 532 (2016) 245–249.
- [40] Y.K. Xiang, F.H. Peng, Y.Q. Guo, et al., Connexin32 activates necroptosis through Src-mediated inhibition of caspase 8 in hepatocellular carcinoma, *Cancer Sci.* 112 (2021) 3507–3519.
- [41] S.Y. Lee, S. Kim, Y. Song, et al., Sorbitol dehydrogenase induction of cancer cell necroptosis and macrophage polarization in the HCC microenvironment suppresses tumor progression, *Cancer Lett.* 551 (2022) 215960.
- [42] X. Tong, R. Tang, M. Xiao, et al., Targeting cell death pathways for cancer therapy: recent developments in necroptosis, pyroptosis, ferroptosis, and cuproptosis research, *J. Hematol. Oncol.* 15 (2022) 174.
- [43] E. Delangre, E. Oppliger, S. Berkcan, et al., S100 proteins in fatty liver disease and hepatocellular carcinoma, *Int. J. Mol. Sci.* 23 (2022).
- [44] C. Sobolewski, D. Abegg, F. Berthou, et al., S100A11/ANXA2 belongs to a tumour suppressor/oncogene network deregulated early with steatosis and involved in inflammation and hepatocellular carcinoma development, *Gut* 69 (2020) 1841–1854.
- [45] M.X. Zhang, W. Gan, C.Y. Jing, S.S. Zheng, Y. Yi, J. Zhang, et al., S100A11 promotes cell proliferation via P38/MAPK signaling pathway in intrahepatic cholangiocarcinoma, *Mol. Carcinog.* 58 (2019) 19–30, <https://doi.org/10.1002/mc.22903>.
- [46] R. Li, J. Gong, C. Xiao, et al., A comprehensive analysis of the MAGE family as prognostic and diagnostic markers for hepatocellular carcinoma, *Genomics* 112 (2020) 5101–5114.
- [47] J.C. Guo, Y.J. Yang, J.Q. Zhang, et al., microRNA-448 inhibits stemness maintenance and self-renewal of hepatocellular carcinoma stem cells through the MAGEA6-mediated AMPK signaling pathway, *J. Cell. Physiol.* 234 (2019) 23461–23474.
- [48] X. Jin, Y. Pan, L. Wang, et al., MAGE-TRIM28 complex promotes the Warburg effect and hepatocellular carcinoma progression by targeting FBP1 for degradation, *Oncogenesis* 6 (2017) e312.
- [49] D. Yu, B. Green, A. Marrone, et al., Suppression of CYP2C9 by microRNA hsa-miR-128-3p in human liver cells and association with hepatocellular carcinoma, *Sci. Rep.* 5 (2015) 8534.
- [50] C.N. Tsai, S.C. Yu, C.W. Lee, et al., SOX4 activates CXCL12 in hepatocellular carcinoma cells to modulate endothelial cell migration and angiogenesis in vivo, *Oncogene* 39 (2020) 4695–4710.
- [51] M. Sandbothe, R. Buurman, N. Reich, et al., The microRNA-449 family inhibits TGF- β -mediated liver cancer cell migration by targeting SOX4, *J. Hepatol.* 66 (2017) 1012–1021.
- [52] J.K. DiStefano, B. Davis, Diagnostic and prognostic potential of AKR1B10 in human hepatocellular carcinoma, *Cancers* 11 (2019).
- [53] T. Wu, Y. Ke, H. Tang, et al., Fidarestat induces glycolysis of NK cells through decreasing AKR1B10 expression to inhibit hepatocellular carcinoma, *Mol Ther Oncolytics* 23 (2021) 420–431.
- [54] R.D. Leone, L. Zhao, J.M. Englert, et al., Glutamine blockade induces divergent metabolic programs to overcome tumor immune evasion, *Science* 366 (2019) 1013–1021.
- [55] A. Kaczmarek, P. Vandenabeele, D.V. Krysko, Necroptosis: the release of damage-associated molecular patterns and its physiological relevance, *Immunity* 38 (2013) 209–223.
- [56] C.J. Kearney, S.J. Martin, An inflammatory perspective on necroptosis, *Mol Cell.* 65 (2017) 965–973.
- [57] T. Zhang, C. Yin, A. Fedorov, et al., ADAR1 masks the cancer immunotherapeutic promise of ZBP1-driven necroptosis, *Nature* 606 (2022) 594–602.